Chinese Chemical Letters 33 (2022) 4640–4644

Contents lists available at ScienceDirect

Chinese Chemical Letters

journal homepage: www.elsevier.com/locate/cclet

Covalent carbene modification of 2D black phosphorus

Lei Zhang[a,b], Zhe-Ji Wang[a], Bo Ma[a], Xiang-Yang Li[a], Yu-Chi Dai[a], Guowen Hu[a], Yong Peng[c], Qiang Wang[a,b,*], Hao-Li Zhang[a,d,*]

[a] State Key Laboratory of Applied Organic Chemistry (SKLAOC), Key Laboratory of Special Function Materials and Structure Design (MOE), College of Chemistry and Chemical Engineering, Lanzhou University, Lanzhou 730000, China
[b] Office of Laboratory and Equipment Management, Lanzhou University, Lanzhou 73000, China
[c] Key Laboratory of Magnetism and Magnetic Materials of Ministry of Education, School of Physical Science and Technology, Lanzhou University, Lanzhou 730000, China
[d] Tianjin Key Laboratory of Molecular Optoelectronic Sciences, Department of Chemistry, Collaborative Innovation Center of Chemical Science and Engineering (Tianjin), Tianjin University, Tianjin 300072, China

ARTICLE INFO

Article history:
Received 30 September 2021
Revised 30 October 2021
Accepted 20 December 2021
Available online 24 December 2021

Keywords:
Two-dimensional materials
Black phosphorus
Covalent functionalization
Carbene
Solubility

ABSTRACT

Black phosphorus (BP) has attracted an ever-growing interest due to its unique anisotropic two-dimensional structure, impressive photoelectronic properties and attractive application potential. However, the tools for bandgap engineering and passivation via covalent modification of BP nanosheets remain limited to diazonium salt and nucleophilic addition methods, so that developing new modification strategies for BP nanosheets is crucial to explore its physical and chemical properties and enrich the toolbox for functionalization. Herein, we report the covalent modification of liquid-phase exfoliated BP nanosheets based on a rational analysis of BP structure. The modification of BP is achieved *via* carbene, a highly reactive organic mediate. The carbene modification improves the solubility and stability of BP nanosheets. Detailed microscopic and spectroscopic characterizations including infrared spectra, Raman spectra, X-ray photoelectron spectra, SEM and TEM were conducted to provide insights for the reaction. The proof of the existence of covalent bonds between BP nanosheets and organic moieties confirms the successful modification. Moreover, theoretical calculations were conducted to unveil the reaction mechanism of the two different types of bonds and the chemical property of two-dimensional BP.

With a unique atomic-thick plane, two-dimensional (2D) materials have garnered ever-growing attention due to their promising application potential in electronics, optics and bio-medicines over the past two decades [1–3]. From the first discovered graphene to transition metal dichalcogenide (TMDs), the element components have been much enriched [4–6]. In 2014, the resurgence of black phosphorus (BP) [7,8], broadened the mono-elemental 2D material family. BP has earned numerous interests owing to its layer-dependent direct bandgaps from 0.3 eV to 2.0 eV, ultrahigh carrier mobility up to 1000 $cm^2\ V^{-1}\ s^{-1}$, impressive on/off ratio (*ca.* 10^5), and anisotropy, emerging as a desirable candidate in the next generation of optoelectronics, energy-storage and nano-machine devices [8–11].

Hitherto, the preparation of BP nanosheets is mainly based on top-down methods including mechanical cleavage [12], ion intercalation [13], electrochemical approach [14] and liquid-phase exfoliation. The mechanical cleavage was introduced to prepare BP nanosheets in 2014 [7], which is usually time-consuming and costly in scale-up production. The intercalation production of BP nanosheets generally suffers from low yield. Electrochemical exfoliation can obtain BP nanosheets in scale but it is prone to be oxidized. Liquid-phase exfoliation (LPE) so far is the most widely utilized method to fabricate BP nanosheets in the laboratory [15].

The ability to covalently modify 2D materials employing various reactive intermediates expands new horizons and extensive opportunities to control and tailor their physical and chemical properties on several designed occasions [16,17]. Based on the well-established organic reactions, the covalent modification of sp^2 hybridized carbon atoms in graphene has greatly expanded the family of graphene derivative materials [18]. Moreover, modification

* Corresponding authors at: State Key Laboratory of Applied Organic Chemistry (SKLAOC), Key Laboratory of Special Function Materials and Structure Design (MOE), College of Chemistry and Chemical Engineering, Lanzhou University, Lanzhou 730000, China.
E-mail addresses: qiangwang@lzu.edu.cn (Q. Wang), haoli.zhang@lzu.edu.cn (H.-L. Zhang).

https://doi.org/10.1016/j.cclet.2021.12.046
1001-8417/

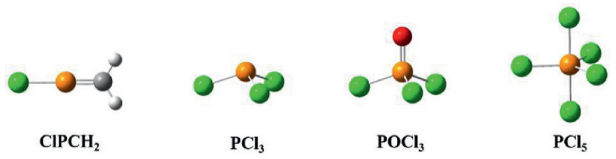

Scheme 1. The common stereochemical configurations of phosphorus-related compounds. The hybridization is sp^2, sp^3, sp^3 and sp^3d, respectively.

plays an important role in regulating the physical and chemical properties of 2D materials. The covalent modification of graphene can open its bandgap while the covalent modification of TMDs usually improves its dispersity and tunes its electronic property [20,19]. Analogously, the covalent modification of BP has followed the footsteps of graphene and TMDs with some delay. Recent works have demonstrated that covalent functionalization and self-assemble methods can effectively improve the stability, and gas sensor performance of BP [10,11].

Although significant efforts have been made to the field of modification of BP, to date, the toolbox to modify BP nanosheets remains rare [17,20]. General methods including diazonium salt modification [21] and nucleophilic addition [22] are all based on the P-C single bond to modify liquid phase exfoliated BP nanosheets. Different from the mechanical exfoliated BP nanosheets on the substrate [23], the reactivity of liquid-phase exfoliated BP nanosheets to diazonium salts displayed an undesirable result [22,24]. Despite diazonium modification gaining success in graphene, the lattice structure of BP is not as flat as graphene, in which the π electrons are delocalized within the entire planer network. The P atoms in BP are sp^3 hybridized thus leaving a lone pair of electrons out of the puckered plane [25]. As a result, the poor reactivity of BP to diazonium salt is expected. To improve the reactivity, we introduced negatively charged BP nanosheets in our previous work [13]. Although the degree of functionalization is improved, the low yield in the intercalation step to produce BP nanosheets hinders its further development and the introduction of *n*-butyl lithium poses safety issues. To date, the LPE method is still the most utilized low cost and mass scalable approach to preparing BP nanosheets. Hence a general modification to the liquid-phase exfoliated route through rational design is highly desired and urgently required. Developing an efficient covalent modification method based on liquid-phase exfoliated BP nanosheets is therefore of great importance.

Herein, we utilized carbene to modify liquid-phase exfoliated BP nanosheets for the first time and explored the reaction products. The modifications of carbon nanomaterials with carbene, mainly on carbon nanotubes [26] and graphene [27], have been proven to be effective. The two unpaired electrons in carbene may interact with the lone pair of electrons in P atoms of BP to form P=C double bonds [28–30]. Meanwhile, the stereochemistry of phosphorus in organic chemistry diversifying from 3-connected to 6-connected enlightened us as well. Among these classic organic phosphorus compounds, two special compounds drew our attention, which are phosphorus trichloride (PCl_3) and phosphorus oxychloride ($POCl_3$) (Scheme 1). In these compounds, the central phosphorus atoms are both sp^3 hybridized, similar to the hybridization of BP. As the P atoms are sp^3 hybridized in the original BP, which is similar to the hybridization of the P atoms in PCl_3, the structure of $POCl_3$ implies that it is possible to modify P atoms through double bonds while the hybridization of P atoms is maintained. Unlike the P-C single bonds realized in previous reports or P=N double bonds via nitrene modification, to the best of our knowledge, P=C double-bond modification has not been previously reported.

Liquid-phase exfoliated BP nanosheets were chosen as starting material herein as LPE is the most utilized strategy to prepare

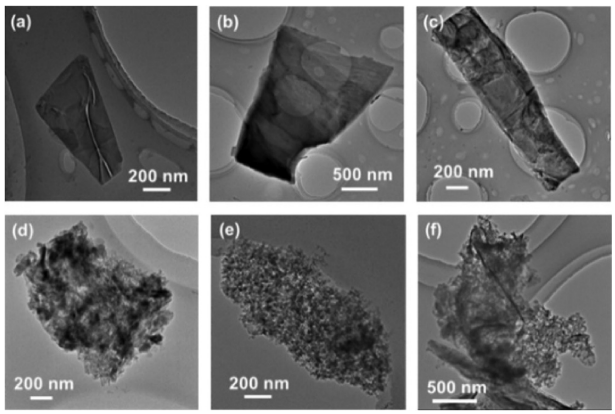

Fig. 1. The TEM images of (a-c) pristine BP nanosheets and (d-f) BP=CCl_2–1.

BP nanosheets. In detail, bulk BP crystal was first fine grounded into powder and then sonicated in N-methyl pyrrolidone (NMP) for 36 h. The suspension was then centrifuged at a rate of 3000 rpm for 10 min to remove the unexfoliated bulk and at 15,000 rpm centrifugation speed for 20 min to collect the precipitate. To produce dichlorocarbene, chloroform ($CHCl_3$) was selected as a precursor with the addition of sodium hydroxide (NaOH). Dichlorocarbene was *in-situ* prepared through α-elimination under basic conditions. The reaction was performed in a mixture of water and chloroform under argon atmosphere while the triethylbenzylammonium chloride was utilized as phase transfer catalyst (PTC) to improve the reactivity. At first, the amount of $CHCl_3$ was 200 μL (2.48 mmol) while the amount of liquid phase exfoliated BP nanosheets was 6 mg (0.19 mmol). After 24 h of reaction, the product was collected and washed several times to remove any physically absorbed organic moieties, abbreviated to BP=CCl_2–1.

BP nanosheets prepared through LPE were characterized by transmission electron microscopy (TEM) for comparison. A flat sheet-like morphology was detected in the pristine sample (Figs. 1a–c), indicating the successful exfoliation of BP bulk in the first step. The pristine BP nanosheets displayed a lattice fringe of 0.256 nm in the high-resolution TEM (HR-TEM) image, which is assigned to the (111) planes of the BP crystal (Fig. S1a in Supporting information). After carbene modification, the product was also characterized through TEM and the results were illustrated in Figs. 1d–f. The morphology of BP=CCl_2–1 is highly irregular after the modification reaction as the typical flat sheet structure cannot be observed anymore. Considering the protection of the argon atmosphere during the reaction, the amorphous structure indicated that the reaction was too intense and the lattice structure of BP has been significantly damaged.

Further Raman spectra results prove the conjecture as well since no Raman signals assigned to BP can be detected in Fig. S2 (Supporting information). Therefore, the amount of $CHCl_3$ was then decreased to 100 μL in order to weaken the high reactivity, and the product was collected under the same aftertreatment. The infrared (IR) spectra were then carried out (Fig. S3 in Supporting information). Compared with the origin BP bulk and pristine BP nanosheets, no obvious peaks located around 700 cm^{-1} representing the vibration of P-C bonds appeared. Moreover, the signal fingered to P=C bonds stretching vibration around 1200 cm^{-1} was affected by the P=O bonds at 1260 cm^{-1} and turned out to be dubious. These facts indicate that the reaction between carbene and BP nanosheets is hard to control and detect. The amount of $CHCl_3$ strongly influenced the degree of modification, whether a severe or mild reaction cannot obtain a satisfying result.

To further optimize the reaction, tetramethylammonium hydroxide ($(CH_3)_4NOH$) was employed to produce carbene instead of

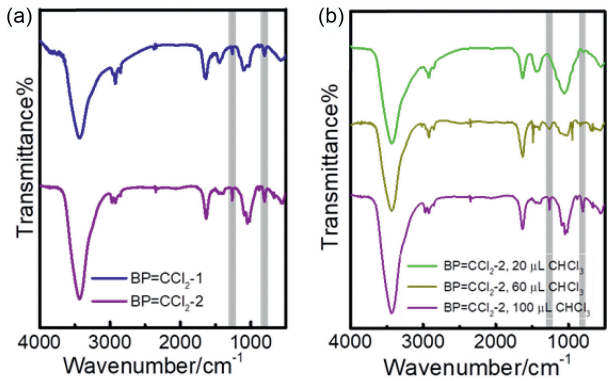

Fig. 2. (a) IR spectra of BP=CCl_2–1 (blue) and BP=CCl_2–2 (purple), respectively. (b) IR spectra of BP=CCl_2–2 prepared with different amount of $CHCl_3$. The volume of $CHCl_3$ is 20 μL (green), 60 μL (brown) and 100 μL (purple), respectively.

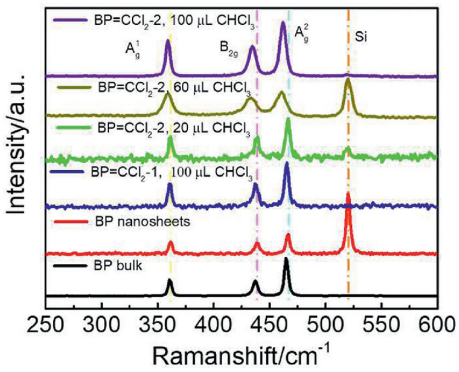

Fig. 3. Raman spectra of BP bulk (black), BP nanosheets (red) and BP=CCl_2–2 prepared with different amounts of $CHCl_3$. The volume of $CHCl_3$ is 20 μL (green), 60 μL (brown) and 100 μL (purple), respectively.

NaOH. The solvent is also changed from a mixture of water and chloroform to tetrahydrofuran (THF), which makes the reaction homogeneous and thus PTC was abandoned. The product was abbreviated to BP=CCl_2–2 and the amount of $CHCl_3$ was controlled as 100 μL, 60 μL and 20 μL, respectively. Under the same amount of $CHCl_3$ (100 μL), compared with IR spectra of BP=CCl_2–1, the IR spectrum of BP=CCl_2–2 exhibits stronger responses at 1250 cm^{-1} and 800 cm^{-1}, respectively (Fig. 2a), suggesting a higher degree of modification. Moreover, a weak peak located at 667 cm^{-1} representing the vibration of P-C single bond stretching appears in BP=CCl_2–2, which is less affected by the phosphorus oxide. The three BP=CCl_2–2 products utilizing the different amounts of $CHCl_3$ (100, 60 and 20 μL) were then collected, respectively. The IR spectra of three samples are illustrated in Fig. 2b. The signals in the three samples generally displayed a similar location but with different intensities. In detail, with the increase of carbene, the signals located around 1200 cm^{-1} representing the existence of P=C bonds appear while the signal intensity at 800 cm^{-1} belonging to the P-C bonds is detected in all three samples and the intensity gradually increased.

Raman spectra and SEM characterization were performed as well in Fig. 3 and Fig. S4 (Supporting information), respectively. Signals assigned to A^1g, B_{2g} and A^2g modes around 361.64, 438.84 and 466.85 cm^{-1} can be observed in bulk BP, pristine BP nanosheets and BP=CCl_2–2 respectively with different degrees of modification, implying that the BP structure was maintained after the modification. Moreover, compared with the peak location of pristine BP nanosheets, the three peaks in BP=CCl_2–2 moved to the low-frequency direction while the peaks in bulk BP displayed a blue shift. The blue shift in bulk BP indicates the successful exfoliation of BP bulk to 2D structure and the redshift is consistent with the literature reported covalent modification of BP nanosheets, which is due to the energy increase of the system [13]. Furthermore, a typical 2D structure with a sheet-like shape can be recognized in the TEM and SEM images of BP=CCl_2–2 (Figs. S1 and S4 in Supporting information). All the Raman spectra and SEM results suggest the structural integrity of the BP nanosheets after the chemical reaction.

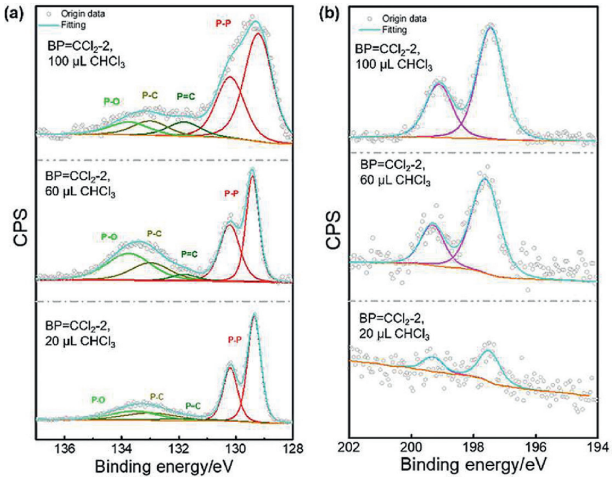

Fig. 4. High resolution (a) P 2p and (b) Cl 2p XPS spectra of BP=CCl_2–2 prepared with different amount of $CHCl_3$. The volume of $CHCl_3$ is 20 μL, 60 μL and 100 μL, respectively.

The above IR spectral results imply the existence of C-P bonds accompanied with C=P bonds. However, the overlap of oxides makes the analysis complicated. To further determine the existence of the organic moieties on the surface, high-resolution X-ray photoelectron spectroscopic (XPS) measurements were carried out. The high-resolution P 2p and Cl 2p XPS spectra of BP=CCl_2–2 were exhibited in Fig. 4. Both P 2p and Cl 2p signals can be tested in the three different samples. Under different volumes of $CHCl_3$ treatments, all samples displayed the doublet peaks at ~130 eV which are assigned to the P $2p_{1/2}$ and P $2p_{3/2}$ levels of BP nanosheets. After the reaction, a broad peak from 131 eV to 135 eV appeared and increased with the increase of $CHCl_3$ amount (Fig. 4a). The broad peak can be deconvoluted into three components including the P-O bonds, P-C bonds and P=C bonds. The intensity of the P=C bond signal increased from 3.51% (BP=CCl_2–2, 20 μL) to 7.48% (BP=CCl_2–2, 100 μL), which is consistent with the degree of modification. This phenomenon indicates that with the increase of carbine amount, heavier modification occurred through P=C bonds. Another proof of the covalent bonded organic moieties on BP nanosheets surface is the response of Cl in BP=CCl_2–2 in the three samples (Fig. 4b). The signals of Cl mainly originate from the carbene, and as the amount of the attached carbene increased, the corresponding Cl signals became stronger.

Transmission electron microscopy (TEM) with element mapping of BP=CCl_2–2 were carried out to determine the surface element information, as shown in Fig. 5. Fig. 5a shows the flat nano-flake structure of the modified BP nanosheets, along with uniform diffraction spots in the selected area electron diffraction (SAED) pattern (Fig. 5b). Lattice fringes were observed in HR-TEM characterization of BP=CCl_2–2, indicating the crystallinity of the nanosheets was maintained after modification (Fig. S1c). In addition, the morphology information of pristine BP nanosheets and BP=CCl_2–2 were studied using atomic force microscopy (AFM). The AFM profile shown in Fig. S5 (Supporting information) displays a typical height less than 15 nm, which confirms the ultrathin feature

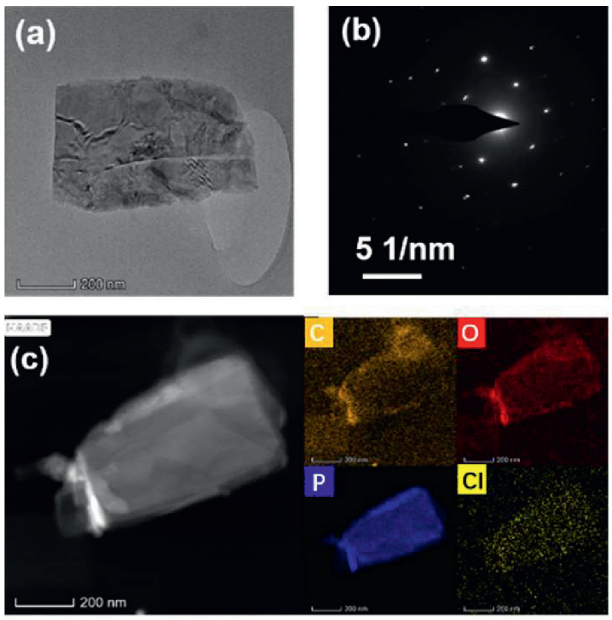

Fig. 5. (a) Transmission electron microscopy (TEM) image; (b) selected area electron diffraction (SAED) pattern; (c) HADDF-STEM images of BP=CCl_2–2 with elemental mapping.

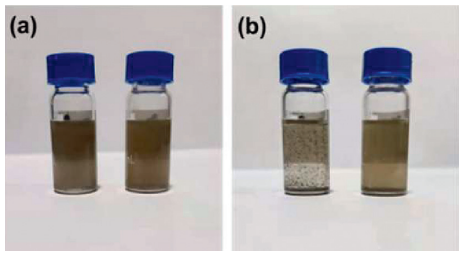

Fig. 6. Dispersibility study of BP nanosheets and BP=CCl_2–2 nanosheets in 1,1,2,2-tetrachloroethane. (a) Photograph of BP nanosheets (left) and BP=CCl_2 nanosheets (right) dispersed at 0 h. (b) Photograph of BP nanosheets (left) and BP=CCl_2 (right) nanosheets dispersed after 5 h.

of BP nanosheets after modification. The TEM and AFM characterizations indicate that the structural integrity of BP was maintained after carbene modification. Moreover, elemental mapping confirms the existence of chloride element, which is dispersed all over the same spatial location where the phosphorus element is located in Fig. 5c.

The solubility improvement of 2D materials with organic moieties on its surface through covalent bonds is the quintessential feature reported in much previous literature [19,31–34]. And the promotion of solubility is crucial to the practical applications of 2D materials in the solution-processable industry. Herein, the solubility of BP=CCl_2–2 was studied and the pristine BP nanosheets were compared as reference. We chose 1,1,2,2-tetrachloroethane as the solvent for its similar structure to BP=CCl_2–2. The result was manifested in Fig. 6. In the beginning, both BP nanosheets and BP=CCl_2–2 nanosheets displayed an acceptable dispersion behavior in 1,1,2,2-tetrachloroethane after sonication. After 5 h, obvious aggregation was observed in the BP nanosheets suspension. In contrast, the dispersion of BP=CCl_2–2 remained homogeneous. A prolonged stability test for 30 days showed gradual decomposition of the pristine BP nanosheets under atmosphere conditions, while no evidence of aggregation or structural damage to the BP=CCl_2–2 nanosheets was observed, confirming the successful surface modification and passivation of BP by carbene (Fig. S6 in Supporting information). The absorption of modified BP nanosheets remained 27% (at 600 nm) after 30 days. Moreover, the TEM results support the conclusion that modification of BP nanosheets improved the stability as well. The typical 2D structure morphology after 30-day ambient exposure was collapsed in pristine BP nanosheets. In contrast, layered-structure can still be observed in modified BP nanosheets (Fig. S1). Pristine BP nanosheets are easily oxidized under ambient atmosphere due to the presence of lone pair electrons rendering the high reactivity with oxygen. As shown above, all the observation from UV-vis spectra and TEM indicated that carbene modification significantly improved the stability of BP nanosheets. Such a stability enhancement can be attributed to the formation of P=C double bonds, which affords five-coordinate bonding of P atoms in BP, thus preventing the reaction to oxygen. These results indicate that the carbene modification method we developed may hold a key to forming stable suspensions of functionalized BP nanosheets in solutions.

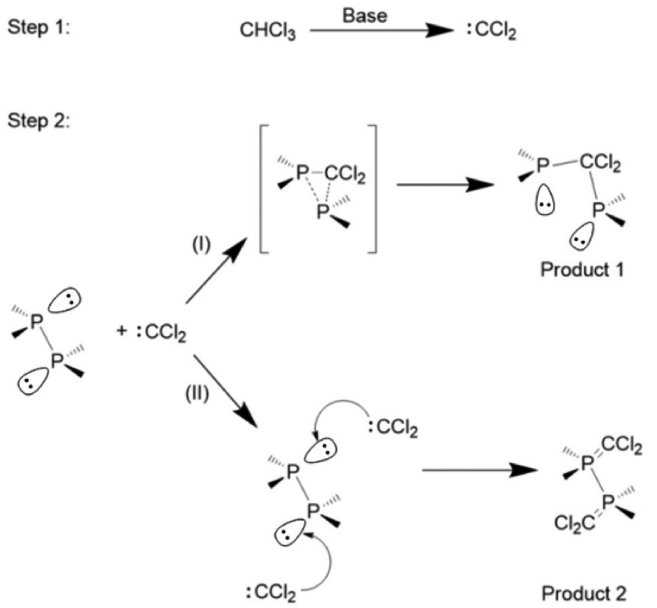

Scheme 2. The proposed mechanism for the reaction between BP nanosheets and $CHCl_3$.

Scheme 2 illustrates a plausible mechanism for the formation of P-C bonds and P=C bonds, which involves two reaction steps. In step 1, carbene was formed through the α-elimination of $CHCl_3$ under mild basic conditions. Then the covalent functional reaction occurs between carbene and the BP nanosheets. Whether the binding is through a single bond or double bonds depends on the amount of carbene. When the amount of carbene is fleabite, the reaction tends to occur between one carbene and two phosphorus atoms thus forming P-C single bonds. With the increase of carbene species, the reaction between one carbene and one phosphorus atom resulting in the formation of P=C double bonds is preferable.

The theoretical simulation was used to provide a further understanding of the reaction mechanism. Firstly, to determine whether the reaction is spontaneous, we assessed the change in the Gibbs energy (ΔG) of the reaction through Eq. 1:

$$\Delta rG^{\ominus} = G_f^{\ominus}(\mathrm{BP{=}CCl_2}) - \left[G_f^{\ominus}(\mathrm{:CCl_2}) + G_f^{\ominus}(\text{BP nanosheets})\right] \quad (1)$$

$G_f^{\ominus}$(BP=CCl_2), $G_f^{\ominus}$(:CCl_2) and $G_f^{\ominus}$(BP nanosheets) stand for the standard Gibbs energies of formation of BP=CCl_2, dichlorocarbene and BP nanosheets, respectively. We simulated three different ratios between dichlorocarbene and BP nanosheets as in our exper-

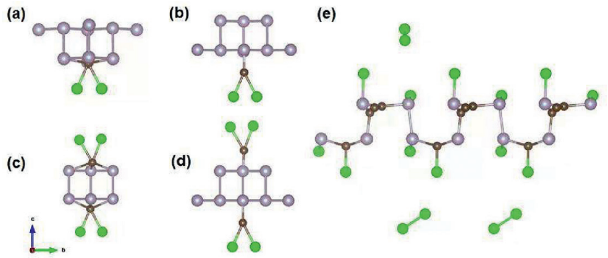

Fig. 7. Theoretically optimized final product structures with different treatment ratios of dichlorocarbene: (a, b) 1:4 (P atom to dichlorocarbene); (c, d) 1:2 (P atom to dichlorocarbene); (e) 1:1 (P atom to dichlorocarbene).

iments (the ratios of P atom to dichlorocarbene are 4:1, 2:1 and 1:1, respectively). Under the ratios of 4:1 and 2:1, both P-C single bond and P=C double bond can be formed. The $\Delta_r G^{\Theta}$ of the final product in the ratio of 4:1 containing P-C bonds is –5.61 eV, lower than that of P=C double bonds (–0.89 eV). However, in the ratio of 2:1 (P atom to dichlorocarbene), the $\Delta_r G^{\Theta}$ of the BP=CCl_2 containing P=C double bonds (–0.36 eV) is lower than that of the P-C single bonds (–0.24 eV). Moreover, with the amount of carbene increasing to the ratio of 1:1, the $\Delta_r G^{\Theta}$ was calculated as –3.71 eV. All the Gibbs energies of formation of the five different types of final products are negative, which indicates that the reaction has a spontaneous tendency. Moreover, the simulated final structures of the five products were demonstrated in Fig. 7. The bonds between P atoms and C atoms can be observed in all products, implying the reaction did occur under all different reactant ratio conditions. However, Fig. 7e also shows that the BP structure is damaged under the 1:1 (P atom to dichlorocarbene) reaction conditions. This result indicates that with a high concentration of dichlorocarbene, further reaction could lead to a structural collapse of BP. The theoretical simulation results match well with the TEM observation, for instance, the BP structure was indeed damaged under the ratio of 1:1 (P atom to dichlorocarbene).

In summary, we demonstrate herein a new surface modification method for liquid phase exfoliated BP nanosheets through reaction with carbene under a homogenous reaction condition without the assistance of the phase transfer catalyst. IR, Raman and XPS characterizations to the products confirmed the successful surface modification to the BP nanosheets. Due to the high reactivity of the carbene, it is crucial to generate the carbene spices under a mild basic condition with an appropriate concentration. A plausible mechanism to explain the formation of P-C single bond and P=C double bond was proposed, which is supported by the theoretical simulation. The solubility and stability of BP nanosheets are significantly improved after carbene modification. It is worth noting that this is the first BP modification method via the formation of C=P double bonds, which realized the five-coordinate bonding of phosphorus element in 2D materials for the first time. This new carbene modification method broadens the toolbox for tailoring the properties of BP nanosheets and opens up the possibility to further functionalization of BP nanosheets with a wide range of desired groups utilizing BP=CCl_2 as a starting platform.

Declaration of competing interest

The authors declare no known competing financial interests or personal relationships that could have appeared to influence the work reported in this paper.

Acknowledgments

This work is supported by the Ministry of Science and Technology of China (No. 2017YFA0204903), National Natural Science Foundation of China (NSFC, Nos. 51733004, 51525303, 22073038, 21702085) and 111 Project. The authors thank beamline BL14B1 (Shanghai Synchrotron Radiation Facility) for providing the beam time. We wish to thank the Electron Microscopy Center of Lanzhou University for the microscopy and microanalysis of our specimens. The theoretical calculation is supported by the Supercomputing Center of Lanzhou University.

Supplementary materials

Supplementary material associated with this article can be found, in the online version, at doi:10.1016/j.cclet.2021.12.046.

References

[1] R. Roldan, L. Chirolli, E. Prada, et al., Chem. Soc. Rev. 46 (2017) 4387–4399.
[2] H. Zhang, ACS Nano 9 (2015) 9451–9469.
[3] H. Huang, J. Zha, S. Li, C. Tan, Chin. Chem. Lett. 33 (2022) 163–176.
[4] J.N. Coleman, M. Lotya, A. O'Neill, et al., Science 331 (2011) 568–571.
[5] A.C. Ferrari, F. Bonaccorso, V. Fal'ko, et al., Nanoscale 7 (2015) 4598–4810.
[6] Z. Zhou, B. Li, C. Shen, et al., Small 16 (2020) 2004173.
[7] L. Li, Y. Yu, G.J. Ye, et al., J. Am. Chem. Soc. 36 (1914) 1344–1363.
[8] J.S. Miao, L. Zhang, C. Wang, 2D Mater. 6 (2019) 032003.
[9] Z. Guo, H. Zhang, S. Lu, et al., Adv. Funct. Mater. 25 (2015) 6996–7002.
[10] C. Qian, R. Wang, M. Li, Colloid. Surf. A Physicochem. Engin. Asp. 608 (2021) 125616.
[11] R. Wang, X. Yan, B. Ge, et al., ACS Sustain. Chem. Engin. 8 (2020) 4521–4536.
[12] M.B. Erande, M.S. Pawar, D.J. Late, ACS Appl. Mater. Interfaces 8 (2016) 11548–11556.
[13] L. Zhang, L.F. Gao, L.X. Li, et al., Mater. Chem. Front. 2 (2018) 1700–1706.
[14] A. Ambrosi, Z. Sofer, M. Pumera, Angew. Chem. Int. Ed. 56 (2017) 10443–10445.
[15] E.A. Lewis, J.R. Brent, B. Derby, S.J. Haigh, D.J. Lewis, Chem. Commun. 53 (2017) 1445–1458.
[16] A. Hirsch, J.M. Englert, F. Hauke, Acc. Chem. Res. 46 (2013) 87–96.
[17] C. Xing, L. Liu, D. Fan, Z. Peng, H. Zhang, FlatChem 13 (2019) 8–24.
[18] G.L. Paulus, Q.H. Wang, M.S. Strano, Mater. Today 19 (2016) 140–145.
[19] K.C. Knirsch, N.C. Berner, H.C. Nerl, et al., ACS Nano 9 (2015) 6018–6030.
[20] S. Thurakkal, X. Zhang, Adv. Sci. 7 (2020) 1902359.
[21] Z. Liu, B. Zhang, N. Dong, J. Wang, Y. Chen, J. Mater. Chem. C 8 (2020) 10197–10203.
[22] Z. Sofer, J. Luxa, D. Bousa, Angew. Chem. Int. Ed. 56 (2017) 9891–9896.
[23] C.R. Ryder, J.D. Wood, S.A. Wells, Nat. Chem. 8 (2016) 597–602.
[24] A. Mitrovic, S. Wild, V. Lloret, Chem. Eur. J. 15 (2020) 3361–3366.
[25] J.R. Brent, N. Savjani, E.A. Lewis, et al., Chem. Commun. 50 (2014) 13338–13341.
[26] Y. Chen, R.C. Haddon, S. Fang, J. Mater. Res. 13 (2011) 2423–2431.
[27] C.K. Chua, A. Ambrosi, M. Pumera, Chem. Commun. 48 (2012) 5376–5378.
[28] J. Sturala, A. Ambrosi, Z. Sofer, M. Pumera, Angew. Chem. Int. Ed. 5 (2018) 14837–14840.
[29] T. Mou, B. Wang, ACS Omega 3 (2018) 2445–2451.
[30] Y. Liu, P. Gao, T. Zhang, et al., Angew. Chem. Int. Ed. 58 (2019) 1479–1483.
[31] K. Zhou, J. Liu, P. Wen, Y. Hu, Z. Gui, Appl. Surf. Sci. 316 (2014) 237–244.
[32] R.H. Goncalves, R. Fiel, M.R. Soares, et al., Chem. Eur. J. 21 (2015) 15583–15588.
[33] S. Eigler, A. Hirsch, Angew. Chem. Int. Ed. 53 (2014) 7720–7738.
[34] Y. Zhu, A.L. Higginbotham, J.M. Tour, Chem. Mater. 21 (2009) 5284–5291.